# Low Complexity Blind Carrier Phase Recovery for Probabilistically Shaped QAM

Gabriele Di Rosa and André Richter, *Senior Member, IEEE*

***Abstract*— We propose a novel two-stage blind carrier phase recovery scheme tailored for probabilistically shaped QAM. Our algorithm is based on modifying the classic Viterbi&Viterbi (V&V) and maximum likelihood (ML) phase estimators by optimizing the blind decisions over the received symbols taking into account the probability distribution of the received signal. Our technique improves the standard V&V + ML in all conditions and outperforms the state-of-the-art blind phase search (BPS) algorithm for a constellation entropy ≤4. At the same time our implementation preserves the low complexity of standard V&V + ML. This results in a remarkable reduction in complexity of up to a factor thirty compared to BPS.**

***Index Terms*— Digital signal processing (DSP), carrier phase recovery, probabilistic shaping, low complexity DSP, Viterbi and Viterbi algorithm, blind phase search.**

## I. Introduction

PROBABILISTIC shaping (PS) has gained increasing popularity in the last years, proving to provide superior performance for coherent transmission over an additive white Gaussian noise (AWGN) channel while enhancing at the same time the transmission rate flexibility. Nevertheless, the theoretical gain predicted with respect to unshaped quadrature amplitude modulation (QAM) is threatened by additional penalties arising from the digital signal processing (DSP) chain, whose adaptation to the peculiar symbol probability distributions of PS constellations is still an under-investigated topic [1]. The practical solutions implemented at the moment are (i) to use modulation-independent heavily pilot-based DSP [2] or (ii) to apply standard blind algorithms developed for unshaped M-QAM. The former choice achieves the best flexibility but at the cost of a consistent reduction in the throughput due to the high pilot overhead (OH). On the contrary, the latter preserves the throughput but is a sub-optimal approach which can introduce consistent penalties [1], [3]. To solve this problem, blind PS-aware algorithms have been developed for polarization demultiplexing and equalization [3] and for frequency offset estimation [4] but, to the best of our knowledge, a PS-aware carrier phase recovery (CPR) has not been proposed yet.

In the context of blind carrier phase estimation (CPE) it is well accepted that the state-of-the-art for high order modulations is represented by the blind phase search (BPS) algorithm [5]. Nevertheless, it has been extensively shown how the interplay between PS and BPS deteriorates the phase estimation, in particular for moderate to low signal-to-noise ratio (SNR) [1]. Moreover, BPS is indisputably an heavily computationally expensive algorithm because of the high number of test rotations that are needed to be performed. This necessity implies either an hardware intensive parallel implementation or slower operations when using a pipelined structure. Efforts have been made to relax the number of needed test rotations, for instance by combining BPS with a second CPE stage [6] or by filtering the phase noise estimator [7]. However, still considerably lower complexity solutions based on the simple Viterbi and Viterbi $4^{th}$ power (V&V) and maximum likelihood phase estimators (ML) have been successfully implemented for unshaped modulation up to 16-QAM [8]. Moreover, these schemes have shown reasonable performance also when applied to 64-QAM [9]. Nevertheless, all these algorithms rely on decisions over the received symbols and amplitudes, whose accuracy is severely impacted by PS if standard Euclidean distance is used as the metric for their discrimination.

We propose a two-stage CPR based on a modification of V&V and ML in which we utilize the knowledge about the a-priori transmitted symbol probabilities to perform optimum symbol and amplitude level assignments. We test our algorithm with variable constellation entropy, ranging from 2.66 to 4.5, and observe that our method outperforms BPS for entropy ≤4 and standard non PS-aware V&V + ML in all conditions, with negligible additional complexity needed.

## II. Algorithm Description

Stage 1: The first stage of our CPR implementation consists of a V&V $4^{th}$ power CPE. The $4^{th}$ power operation allows to properly remove the modulation from 4-QAM modulated signals. When applying the algorithm to high order constellations, amplitude discrimination over the received symbols must be performed in order to consider only symbols which belong to the 4-QAM like amplitude rings [9]. Considering for the phase estimation other symbols increases the estimation error and it is thus needed to minimize the number of erroneous amplitude level assignments to the received complex symbols. While for unshaped QAM a simple yet effective discriminating threshold is obtained by minimizing the Euclidean distance between the received symbol's amplitude and the ideal constellations rings, this choice becomes particularly sub-optimal for PS-QAM. The optimum discrimination can be obtained by maximizing

Manuscript received June 15, 2020; revised July 7, 2020; accepted July 23, 2020. Date of publication July 30, 2020; date of current version August 11, 2020. This work was supported in part by the European Union (EU) through the H2020-MSCA-ITN-2018 Grant Agreement 814276 (WON) and in part by the German Ministry of Education and Research under Grant 16KIS0993 (OptiCON). *(Corresponding author: Gabriele Di Rosa.)*

The authors are with VPIphotonics GmbH, 10587 Berlin, Germany (e-mail: gabriele.di.rosa@vpiphotonics.com; andre.richter@vpiphotonics.com).

Color versions of one or more of the figures in this letter are available online at http://ieeexplore.ieee.org.

Digital Object Identifier 10.1109/LPT.2020.3012970

the probability that the received symbol with amplitude $A$ belongs to the $k$-th constellation ring $R_k$ among the possible $K$ amplitude levels. In other terms the optimum constellation ring assignment is performed as:

$$\max_k \left(f(R_k|A)\right) \iff \max_k \left(f(R_k)f(A|R_k)\right), \qquad (1)$$

where the logical equality follows from Bayes theorem and $f(\cdot)$ indicates probability density function (PDF). Here $f(R_k)$ is known a-priori given a specific PS-QAM constellation. Knowing the noise variance $\sigma^2$ due to AWGN impairing the received signal we can then write:

$$f(A|R_k) = \frac{A}{\sigma^2}\exp\left[\frac{-(A^2+R_k^2)}{2\sigma^2}\right] I_0\left(\frac{AR_k}{\sigma^2}\right), \qquad (2)$$

where $I_0(\cdot)$ is the $0^{th}$ order modified Bessel function. For a given constellation entropy and estimated SNR the maximization can be performed a-priori by defining the thresholds among different rings $R_k, R_{k+1} (k = 1 \ldots K-1)$ as proposed in [3]. These values can be stored for the desired SNR range and granularity in a look-up table (LUT) for an efficient real-time implementation. The knowledge of the SNR is required for the proper choice of the thresholds, but at this stage of the coherent receiver's DSP chain SNR estimation is usually included for performance monitoring [10]. The additional LUT represents then the only supplementary hardware block needed with respect to the standard V&V implementation.

Stage 2: The phase estimation can be refined through an additional ML stage [6]. Here the phase error over a block of $N$ received complex symbols $y_i$ , $i = 1, .., N$ is estimated as:

$$\theta_{ML} = \arg\left(\mathrm{Im}(z)/\,\mathrm{Re}(z)\right), \quad z = \sum_{i=1}^{N} y_i \cdot x_i^*, \qquad (3)$$

where $x_i$ is the blind decision over the $i^{th}$ symbol prior to the application of the ML. For unshaped QAM all the constellation points have the same transmission probability and minimizing the Euclidean distance of the received complex symbols to the ideal constellation points is well known to be the optimum decision method in presence of AWGN noise. On the contrary, for PS-QAM an optimum maximum a posteriori probability (MAP) detection has been proposed [11]. Following this approach symbol decisions are performed as:

$$\min_j ||y_i - x_j||^2 - 2\sigma^2 \ln\left[f(x_j)\right], \quad j = 1 \ldots . M. \qquad (4)$$

This approach is used for our ML stage and proves effective in reducing the number of symbol classification errors, in particular for low SNR. The same implementation strategy proposed for the previous stage, consisting in storing SNR-dependent thresholds in a LUT, can be applied also in this case. In section V we study the dependence of the decision algorithms used in the two stages on the accuracy of the estimated SNR. This allows us to understand the needed LUT granularity and the required SNR estimation accuracy, thus providing useful information about the additional hardware implementation cost of our method.

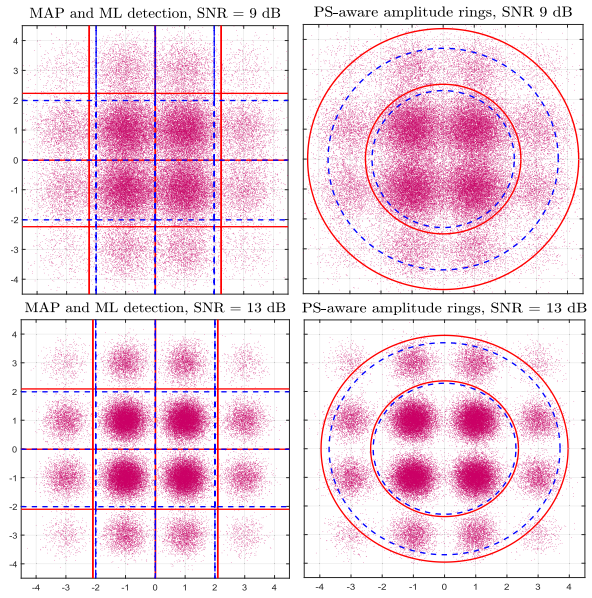


Fig. 1. Decision regions over a 16-QAM-PS constellation with 3.33 target entropy impaired by AWGN with SNR = 9 dB (top) and 13 dB (bottom). On the left side comparison between ML (blue, dashed) and MAP (red, solid) symbol detection. On the right thresholds for PS-aware (red,solid) and standard Euclidean distance based (blue,dashed) amplitude ring assignment.

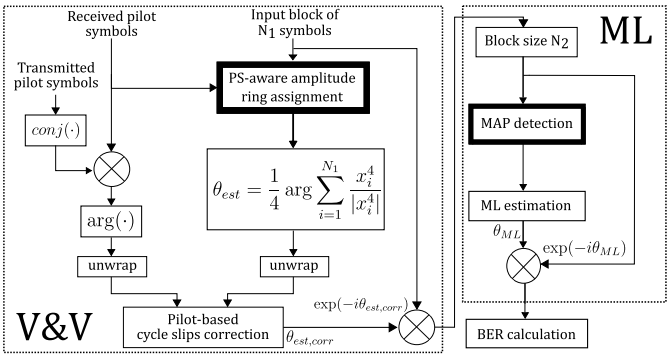


Fig. 2. Block diagram of the proposed two-stage CPR.

In Fig. 1 we can observe the impact of the optimized PS-aware decision metrics on the thresholds for a 16-QAM-PS constellation with 3.33 target entropy (16-QAM-PS3.33) shaped following a Maxwell-Boltzmann probability mass function (PMF). It is evident that the thresholds of the inner constellation rings are increased due to the higher occurrence probability of low-amplitude symbols. Secondly, Fig. 1 reveals that the thresholds are more strongly shifted for lower SNR. This is due to the fact that the Rician PDF, which describes the received symbols' amplitude probability in (2), tends towards a Gaussian PDF with decreasing noise variance. In this case the standard Euclidean distance based thresholds converge to the ones obtained considering PS-QAM.

## III. Algorithm Implementation

To assess the performance of the proposed algorithm we implement and compare it to standard V&V + ML and BPS. In Fig. 2 the block diagram detailing our implementation is shown. Here, the blocks with a thicker black frame are the ones that differ with respect to the standard non PS-aware

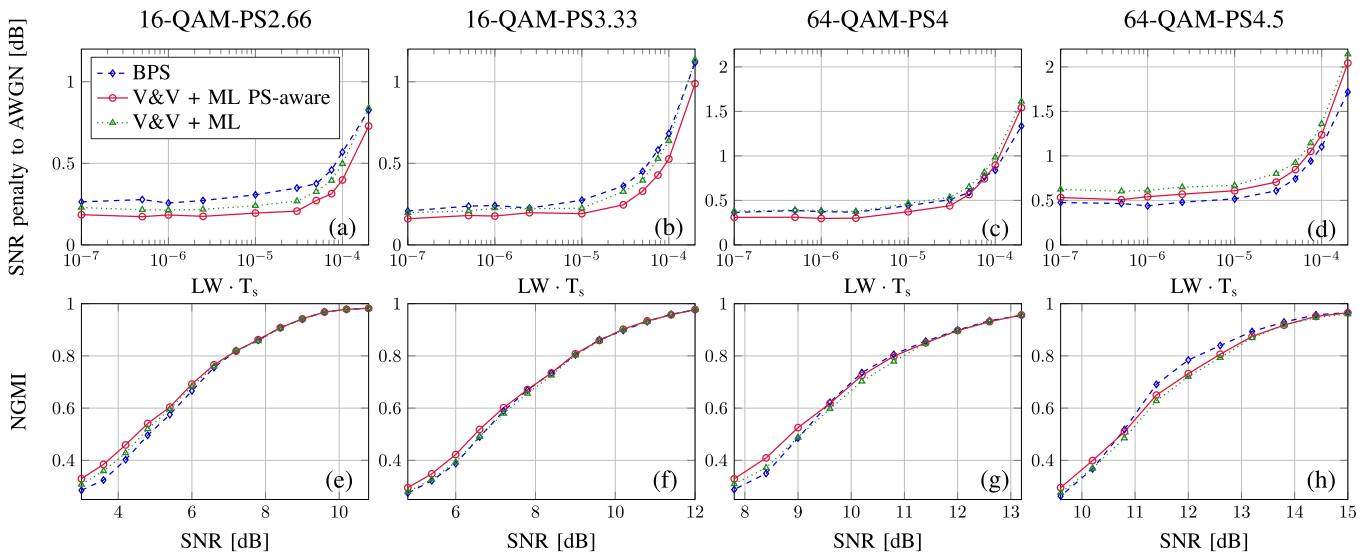


Fig. 3. Top: SNR penalty of the implemented algorithms with respect to AWGN for BER $= 2.7 \times 10^{-2}$ versus the combined linewidth symbol-duration product. The AWGN SNR values considered are: $\mathrm{SNR}_{0,2.66} = 7.35$ dB, $\mathrm{SNR}_{0,3.33} = 9.33$ dB, $\mathrm{SNR}_{0,4} = 10.60$ dB, $\mathrm{SNR}_{0,4.5} = 12.05$ dB. Bottom: NGMI versus SNR for $\mathrm{LW} \cdot \mathrm{T_s} = 10^{-5}$, equivalent to a combined linewidth of 320kHz considering 32 Gbaud signals.

V&V + ML. Together with the phase estimation, we include to all the algorithms a low-OH pilot-based cycle slips (CS) detection and correction unit. This allows us to realistically take into account the effect of CS on the different CPR schemes. A maximum OH of 1% is set for this purpose since it proved to guarantee a CS-free output in all our simulated scenarios while keeping reasonably low the throughput penalty compared to fully pilot-based approaches. These pilot symbols are shaped following the PMF of the transmitted signal in order to avoid altering the total constellation entropy. Concerning the actual CPE, we implement block-averaged filters for all three algorithms to keep the complexity low. The block length of the different stages is then optimized as in [9] by maximizing the laser's linewidth tolerance for a given SNR penalty with respect to the AWGN case. For entropy $\leq$4 a penalty threshold of 0.5 dB is chosen while 1 dB is considered for entropy $>$4. This optimization is performed for a target hard-decision bit error rate (BER) of $2.7 \times 10^{-2}$, assuming 20% forward error correction OH (FEC-OH) [12].

## IV. Simulation Setup and Results

We simulate the transmission of $2^{16}$ symbols modulated as 16-QAM-PS or 64-QAM-PS with variable entropy, ranging from 2.66 to 4.5. The received signal is then corrupted by AWGN in order to simulate the effect of optical amplifiers in the link and by phase noise. The latter is modeled as a Wiener process and reproduces the effect of the combined linewidth of the lasers of the transmitter and of the local oscillator. For each working point ten different noise realizations are simulated in order to collect an accurate statistics of the algorithms' performance over $\approx$650000 symbols. Fig. 3 (a-d) depict the penalty with respect to the SNR needed for obtaining a BER of $2.7 \times 10^{-2}$ for the specified modulation format in the presence of AWGN only. Evidently, in this scenario our proposed 2-stage CPR outperforms in all conditions its non PS-aware counterpart. Furthermore, we notice a visible improvement also with respect to BPS when considering 16-QAM-PS. Moving towards higher spectral efficiency our scheme still outperforms BPS for 64-QAM-PS with 4 bits/symbol for a reasonably high linewidth symbol-duration product $<10^{-4}$. On the contrary, when the entropy is increased further, BPS shows an increased performance gain, confirming to be the best algorithm for higher order modulation formats. This behavior can be mainly explained by the inability of the V&V $4^{th}$ power algorithm to provide good performance because of the decreasing number of symbols available for the phase estimation. While in fact for 64-QAM-PS4 still $\approx$58% of the symbols fall inside the 4-QAM-like constellation rings, this number rapidly decreases with the entropy, reaching a value of only 18.75% for unshaped 64-QAM. On the contrary, the enhanced penalty of BPS for lower order modulation formats can be justified by considering that such signals contain a strongly reduced number of symbols in the outer points, on which BPS strongly relies for providing accurate phase estimation [1]. In Fig. 3 (e-h) the normalized generalized mutual information (NGMI) is plotted versus SNR for a realistic linewidth symbol-duration product of $10^{-5}$. Our algorithm is only outperformed by BPS in the 4.5 entropy case for high SNR values. At the same time, it shows a clear performance improvement with respect to standard V&V and BPS for low SNR values in all four entropy cases. With decreased noise power the performance of our algorithm approaches the one of standard V&V. This is in agreement with what was qualitatively shown in Fig. 1, where we observed that the thresholds are subject to a more substantial modification for lower SNR values. Concerning the implementation cost, BPS introduces a very high complexity that can be roughly estimated as $B$ times the one of a V&V stage with comparable block length [5], where $B$ is the number of test phases used. Regarding ML it is possible instead to approximate its implementation cost as the one of equivalently calculating two additional test phases for the BPS [6]. The exact CPR parameters used for obtaining the results of Fig. 3 (a-d) are listed in Table I, where the letter $N$ represents the filter's block length. For 16-QAM-PS only 16 test phases

TABLE I
PARAMETERS OF THE DIFFERENT CPR IMPLEMENTATIONS

| Constellation entropy | **2.66** | **3.33** | **4** | **4.5** |
|---|---|---|---|---|
| $N$ V&V | 150 | 130 | 130 | 120 |
| $N$ ML | 50 | 50 | 50 | 50 |
| $N$ BPS | 90 | 90 | 70 | 70 |
| $B$ | 16 | 16 | 64 | 64 |

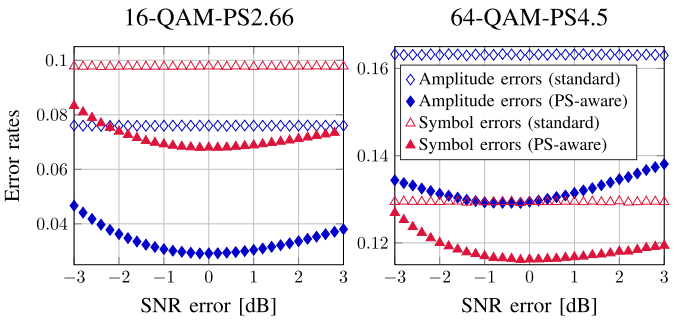


Fig. 4. Error rate of symbols and amplitude rings assignments with standard and proposed PS-aware decisions. The SNR is set to 7.5 dB for 16-QAM-PS2.66 and to 12.5 dB for 64-QAM-PS4.5.

are used for the BPS since increasing this value provided negligible improvement of the performance while strongly affecting the algorithm's complexity. For the analysis in Fig. 3 (e-h) the filter length for V&V and BPS is set to N = 100 in order to provide a fair comparison among algorithms with equal noise rejection capabilities.

## V. DEPENDENCE OF THE ALGORITHM ON SNR ESTIMATION

When discussing our algorithm in Section II, we proposed for a low complexity implementation the use of LUTs to store SNR-dependent thresholds for both symbols and amplitude rings discrimination. Clearly, the hardware cost of this solution is directly proportional to the number of values stored, which is given by the SNR granularity needed for the LUT. Moreover, also if we consider infinitesimal granularity the effectiveness of the method in realistic conditions will depend on the accuracy of the SNR estimation.

To consider these two real-world limitations, we provide incorrect SNR values to our two decision algorithms and observe the impact on their performance, expressed as the error rate of the decisions performed. The results of the analysis are shown in Fig. 4, where we perform this test at the edges of our simulation range, with entropy equal to 2.66 and 4.5 to simulate both, a best- and worst-case scenario. We set SNR = 7.5 dB when considering 16-QAM-PS2.66 and SNR = 12.5 dB for 64-QAM-PS4.5. These values are chosen from Fig. 3 (a-d) as they represent realistic working points.

In Fig. 4 we can observe that the PS-aware decisions outperform the standard ones in all conditions, showing a lower error rate even for a 3 dB error in the estimated SNR. Moreover, we notice a slow gradual increase of the error rate around the optimum value, with the values contained in a $\pm 1$ dB SNR range showing virtually no penalty. We can conclude that our proposed method is robust with respect to both approximate SNR estimation and rounding errors arising from the finite granularity of a coarse LUT.

## VI. CONCLUSION

We presented a novel two-stage blind CPR implementation based on V&V and ML phase estimation tailored over probabilistically shaped QAM. Our algorithm shows a performance gain which increases for decreasing SNR with respect to standard V&V + ML in all simulated scenarios. Moreover, it achieves a visible improvement with respect to the state-of-the-art BPS for 16-QAM-PS while allowing for a tenfold decrease of complexity. When applied to 64-QAM-PS our proposed scheme outperforms BPS as well for a target of 4 bits/symbol. However, except for very low SNR values, if the constellation entropy is further increased BPS proves to be the best performing algorithm. Nevertheless, in these scenarios we are able to partially close the gap with V&V + ML and provide good performance while maintaining a remarkable reduction of the complexity of approximately a factor 30. We verified the robustness of our low-complexity implementation, based on the use of small-sized SNR-dependent LUTs for a given constellation, through additional simulations. We have proven that the algorithm shows very low sensitivity with respect to inaccurate SNR estimations in a realistic range of uncertainty.

## ACKNOWLEDGMENT

The authors gratefully acknowledge Stefanos Dris for his preceding work on the topic of PS-aware DSP techniques.

## REFERENCES

[1] F. A. Barbosa, S. M. Rossi, and D. A. A. Mello, "Phase and frequency recovery algorithms for probabilistically shaped transmission," *J. Lightw. Technol.*, vol. 38, no. 7, pp. 1827–1835, Apr. 1, 2020.
[2] J. Renner *et al.*, "Experimental comparison of probabilistic shaping methods for unrepeated fiber transmission," *J. Lightw. Technol.*, vol. 35, no. 22, pp. 4871–4879, Nov. 1, 2017.
[3] S. Dris, S. Alreesh, and A. Richter, "Blind polarization demultiplexing and equalization of probabilistically shaped QAM," in *Proc. Opt. Fiber Commun. Conf. (OFC)*. Washington, DC, USA: Optical Society America, 2019, pp. W1D–2.
[4] Q. Yan, L. Liu, and X. Hong, "Blind carrier frequency offset estimation in coherent optical communication systems with probabilistically shaped M-QAM," *J. Lightw. Technol.*, vol. 37, no. 23, pp. 5856–5866, Dec. 1, 2019.
[5] T. Pfau, S. Hoffmann, and R. Noe, "Hardware-efficient coherent digital receiver concept with feedforward carrier recovery for $M$-QAM constellations," *J. Lightw. Technol.*, vol. 27, no. 8, pp. 989–999, Apr. 15, 2009.
[6] X. Zhou, "An improved feed-forward carrier recovery algorithm for coherent receivers with $M$-QAM modulation format," *IEEE Photon. Technol. Lett.*, vol. 22, no. 14, pp. 1051–1053, Jul. 15, 2010.
[7] J. R. Navarro *et al.*, "Blind phase search with angular quantization noise mitigation for efficient carrier phase recovery," *Photonics*, vol. 4, no. 2, p. 37, 2017.
[8] J. H. Ke, K. P. Zhong, Y. Gao, J. C. Cartledge, A. S. Karar, and M. A. Rezania, "Linewidth-tolerant and low-complexity two-stage carrier phase estimation for dual-polarization 16-QAM coherent optical fiber communications," *J. Lightw. Technol.*, vol. 30, no. 24, pp. 3987–3992, Dec. 15, 2012.
[9] S. M. Bilal, C. R. S. Fludger, V. Curri, and G. Bosco, "Multistage carrier phase estimation algorithms for phase noise mitigation in 64-quadrature amplitude modulation optical systems," *J. Lightw. Technol.*, vol. 32, no. 17, pp. 2973–2980, Sep. 1, 2014.
[10] Z. Dong, F. N. Khan, Q. Sui, K. Zhong, C. Lu, and A. P. T. Lau, "Optical performance monitoring: A review of current and future technologies," *J. Lightw. Technol.*, vol. 34, no. 2, pp. 525–543, Jan. 15, 2016.
[11] S. Hu *et al.*, "MAP detection of probabilistically shaped constellations in optical fiber transmissions," in *Proc. Opt. Fiber Commun. Conf. (OFC)*. Washington, DC, USA: Optical Society of America, 2019, pp. W1D–3.
[12] E. Agrell and M. Secondini, "Information-theoretic tools for optical communications engineers," in *Proc. IEEE Photon. Conf. (IPC)*, Sep. 2018, pp. 1–5.